Journal of Magnetic Resonance **154,** 130–135 (2002)
doi:10.1006/jmre.2001.2468, available online at http://www.idealibrary.com on IDEAL®

COMMUNICATIONS

NMR Spin Locking of Proton Magnetization under a Frequency-Switched Lee–Goldburg Pulse Sequence

Riqiang Fu,*,[1] Changlin Tian,*,† and Timothy A. Cross*,†,‡

*Center for Interdisciplinary Magnetic Resonance, National High Magnetic Field Laboratory, 1800 E. Paul Dirac Drive, Tallahassee, Florida 32310; and †Department of Chemistry; and ‡Institute of Molecular Biophysics, Florida State University, Tallahassee, Florida 32306

Received March 12, 2001; revised August 30, 2001

The spin dynamics of NMR spin locking of proton magnetization under a frequency-switched Lee–Goldburg (FSLG) pulse sequence is investigated for a better understanding of the line-narrowing mechanism in PISEMA experiments. For the sample of oriented $^{15}N_{1,3,5,7}$-labeled gramicidin A in hydrated DMPC bilayers, it is found that the spin–lattice relaxation time $T_{1\rho}^H$ in the tilted rotating frame is about five times shorter when the ^1H magnetization is spin locked at the magic angle by the FSLG sequence compared to the simple Lee–Goldburg sequence. It is believed that the rapid phase alternation of the effective fields during the FSLG cycles results in averaging of the spin lock field so that the spin lock becomes less efficient. A FSLG supercycle has been suggested here to slow the phase alternation. It has been demonstrated experimentally that a modified PISEMA pulse sequence with such supercycles gives rise to about 30% line narrowing in the dipolar dimension in the PISEMA spectra compared to a standard PISEMA pulse sequence.

Key Words: **frequency-switched Lee–Goldburg (FSLG); PISEMA; spin lock; magic angle.**

With the use of a frequency-switched Lee–Goldburg (FSLG) pulse sequence (*1, 2*) to sufficiently suppress proton homonuclear dipolar coupling, PISEMA (*p*olarization *i*nversion *s*pin *e*xchange at *m*agic *a*ngle) (*3*) has dramatically improved the resolution of static solid-state anisotropic dipolar and chemical shift correlation spectra. The PISEMA experiments have been widely used to obtain orientational constraints from uniformly labeled membrane proteins in a lamellar phase lipid environment (*4–8*). In particular, the resonance patterns in the two-dimensional PISEMA spectra form the so-called PISA wheels (*p*olarity *i*ndex *s*lant *a*ngle) (*9, 10*), which uniquely define the helical tilt with respect to the bilayer normal without a need for resonance assignments. Here the spin dynamics of NMR spin locking of proton magnetization under the FSLG sequence is investigated for a better understanding of the line-narrowing mechanism in the PISEMA experiments.

Cross-polarization (CP) transfer (*11*) of magnetization between the abundant I spin (e.g., ^1H) and the dilute S spin (e.g., ^{15}N) is generally achieved by spin locking both I and S spins with radiofrequency (RF) amplitudes that fulfill the Hartmann–Hahn match condition $\omega_{1I} = \omega_{1S}$ (*12*), where ω_{1I} and ω_{1S} refer to the amplitudes of the RF fields applied to the I and S spins, respectively. Transient dipolar oscillations during the CP transfer have been observed in various systems that exhibit a relatively weak proton–proton coupling network (*13–16*). In these systems, the magnetization M as a function of the spin lock time t can be modeled (*15, 16*) by using the following equation modified from Müller *et al.* (*13*),

$$M(t) = M_0 \exp\left(-t/T_{1\rho}^H\right)\left(1 - 0.5\exp(-Rt) - 0.5\exp(-1.5Rt)\cos\left(\frac{\Delta\nu t}{2}\right)\right), \quad [1]$$

where $T_{1\rho}^H$ is the proton spin–lattice relaxation time in the rotating frame, R refers to the proton spin diffusion rate, and $\Delta\nu$ is the magnitude of the orientation-dependent dipolar interactions between the observed S spin and the directly bonded protons. The oscillation term in the above equation results from the coherent energy transfer between protons and S spins and the oscillation frequency reveals the orientation-dependent heteronuclear interaction. However, the dipolar oscillation is primarily damped by the proton–proton spin diffusion due to the strong coupling of the directly bonded protons with remote protons. As an example, for $^{15}N_{1,3,5,7}$-labeled gramicidin A in hydrated DMPC bilayers, the proton spin diffusion R^{-1} at 9.4 T is about 280 μs (*16, 17*), while the $T_{1\rho}^H$ is on an order of milliseconds (*vide infra*).

In the PISEMA experiment (*3*), the spin exchange between the protons and the S spins occurs during the Hartmann–Hahn match condition when the proton magnetization lies along the magic angle with the RF irradiation of FSLG (*18*), suppressing

[1] To whom correspondence should be addressed. Fax: (850)644-1366. E-mail: rfu@magnet.fsu.edu.

1090-7807/02 $35.00

the strong proton homonuclear dipolar interaction. By analogy to the spin dynamics during cross polarization as in Eq. [1], the spin exchange can be described as (*15, 19*)

$$s(t) = \exp\left(-t/T_{1\rho}^{H}\right)\exp(-1.5Rt)\cos\left(\frac{\sin\theta_M \Delta\nu t}{2}\right), \quad [2]$$

where $T_{1\rho}^{H}$ and R represent the spin–lattice relaxation time and proton spin diffusion rate in the tilted rotating frame, respectively, and $\theta_M = 54.7^\circ$ is the magic angle along which the proton magnetization lies during FSLG. The oscillation frequency is thus scaled by a factor of $\sin\theta_M$. The FSLG sequence sufficiently suppresses the strong proton homonuclear dipolar interaction, resulting in a significant decrease of the proton spin diffusion. Therefore, the decay of the spin exchange oscillation is now governed by the spin–lattice relaxation time $T_{1\rho}^{H}$ in the tilted rotating frame. Consequently, the resulting linewidths in the dipolar dimension are significantly narrower than those obtained in a conventional separated-local-field experiment (*20*) where the linewidths are governed by T_2, which is generally much shorter than $T_{1\rho}^{H}$ in solids. In addition, the coupling with the remote protons contributes more significantly to the linewidths in the separated-local-field experiment than in the PISEMA experiment (*19*). The study here will focus on the spin locking of the proton magnetization under different spin lock schemes, particularly the FSLG sequence, because $T_{1\rho}^{H}$ may be directly associated with the dipolar linewidth in the PISEMA spectra.

A pulse sequence commonly used for indirect $T_{1\rho}^{H}$ measurements is diagrammed in Fig. 1A. In the beginning of the sequence, the ^{1}H magnetization is rotated from the z axis to the y axis in the rotating frame by a 90° pulse and then spin locked along the y axis by a continuous-wave (CW) on-resonance irradiation. Finally, ^{15}N signals are polarized by cross polarization and detected during high-power proton decoupling. Consequently, the proton magnetization as a function of spin lock time t can be indirectly monitored by the ^{15}N signal intensities. In Fig. 1B, the ^{1}H magnetization is initially flipped to the magic angle by a 54.7° pulse and then spin locked by a Lee–Goldburg (LG) sequence (*1*). Here LG_{+Y} refers to an RF pulse with amplitude ω_{1H} applied along the $+y$ direction at the positive offset of $\Delta\omega$ from the ^{1}H resonance lines fulfilling the condition of $\omega_{1H} = \sqrt{2}\Delta\omega$. Thus the effective field of the LG sequence lies along the magic angle. At the end of the spin lock, a 35.3° pulse rotates the ^{1}H magnetization from the magic angle to the y axis followed by ^{15}N detection via cross polarization. Instead of using the LG sequence as in Fig. 1B, a frequency-switched Lee-Goldburg sequence is employed to spin lock the ^{1}H magnetization along the magic angle, as shown in Fig. 1C. For FSLG, each cycle (2τ) consists of two LG units, one of which is applied in the $+y$ direction at the positive offset of $+\Delta\omega$ from the resonance lines (i.e., LG_{+Y}), while the other one is applied in the $-y$ direction at the negative offset of $-\Delta\omega$ from the resonance lines (i.e., $-\mathrm{LG}_{-Y}$). Thus the effective fields of the two LG units have an opposite direction along the magic angle. For each LG unit the effective field has a 2π rotation, i.e., $\tau = 2\pi/\omega_{\mathrm{eff}}$, where $\omega_{\mathrm{eff}} = \sqrt{3}\Delta\omega$.

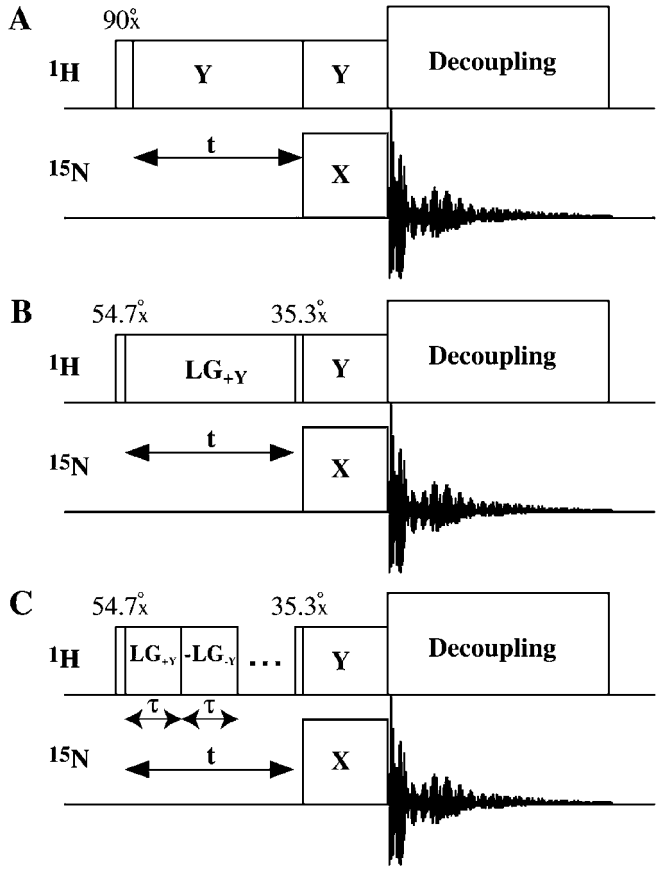

FIG. 1. Pulse sequences used for indirect measurement of $T_{1\rho}^{H}$ relaxation times in different spin lock schemes. (A) Spin lock in the x–y plane by an on-resonance continuous-wave (CW) irradiation. (B) Spin lock at the magic angle by a Lee–Goldburg sequence (LG) (*1*). (C) Spin lock at the magic angle by a frequency-switched Lee–Goldburg (FSLG) sequence.

Gramicidin A (gA) is a polypeptide of 15 amino acid residues, whose high-resolution structure in lipid bilayers has been defined with 120 orientational restraints from solid-state NMR (*21, 22*). Here about 10 mg of $^{15}\mathrm{N}_{1,3,5,7}$-labeled gramicidin A in hydrated (50% by weight) DMPC bilayers (1/8 peptide/lipid molar ratio) oriented with the bilayer normal parallel to the magnetic field direction was used for our measurements. In such an oriented sample, each of these ^{15}N labeled sites contributes to a signal at 198 ppm (*21*). Figure 2 shows the semilog plot of normalized ^{15}N signal intensities versus spin lock time t obtained from the pulse sequences shown in Fig. 1. By fitting the experimental data, it is found that the measured $T_{1\rho}^{H}$ was 3.51 ms at the on-resonance spin lock while it was 7.37 ms by the LG spin lock along the magic angle. In other words, the spin–lattice relaxation process in the tilted rotating frame is about two times slower along the magic angle than in the x–y plane. In fact, the on-resonance RF irradiation scales down the proton homonuclear dipolar interaction by 1/2 (*23*). The residual homonuclear

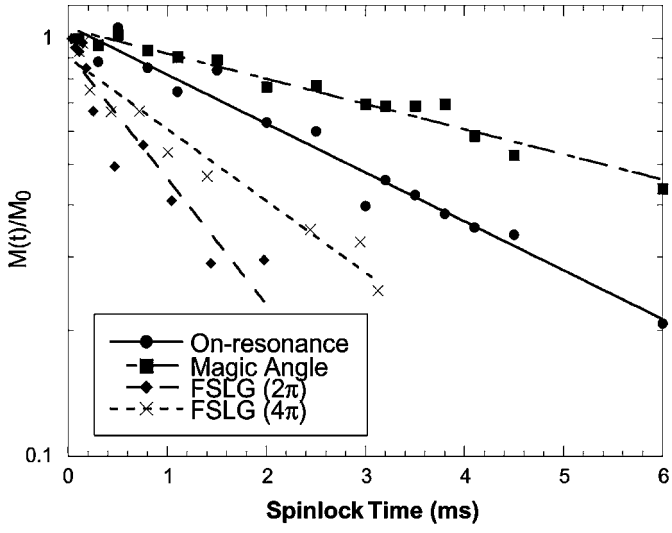

FIG. 2. Semilog plot of normalized magnetization intensities as a function of spin lock time using the pulse sequences diagrammed in Fig. 1. The experiments were performed at 310 K on a homebuilt 400-MHz NMR spectrometer assembled around a Chemagnetics data acquisition system, where the Larmor frequencies for ^{1}H and ^{15}N are 400 and 40 MHz, respectively. The ^{1}H 90° pulse length was 5.5 μs and the resonance offset for the LG sequence was 32.5 kHz. τ was set to 17.96 (i.e., 2π rotation) and 35.92 μs (i.e., 4π rotation), respectively, for the FSLG sequence and 1 μs was used for frequency jump. All experiments used a cross-polarization period of 800 μs with a recycle delay of 7 s. The ^{1}H spin–lattice relaxation time $T_{1\rho}^H$ obtained by fitting the experimental data, as indicated by the lines, was 3.51, 7.37, 1.44, and 2.53 ms for spin lock at on-resonance, at the magic angle by LG, and by FSLG with 2π and 4π rotations, respectively.

dipolar interaction in the rotating frame is commuted with the RF field and thus does not contribute to the decay of the magnetization in the rotating frame. However, the high-order homonuclear dipolar interaction (not commuted with the RF field) may result in decay of the ^{1}H magnetization along the spin lock field, particularly in a relatively weak RF irradiation. In our experiments, the RF amplitude used was just 45.5 kHz, comparable with the homonuclear dipolar interaction in the system studied here. On the other hand, the RF field at the magic angle, to the first order, completely suppresses the strong proton homonuclear dipolar interaction so that the spin lock field becomes much larger than residual internal interactions in the spin system, thus resulting in a slow $T_{1\rho}^H$ process.

Surprisingly, when the ^{1}H magnetization along the magic angle was spin locked by the FSLG sequence, the measured $T_{1\rho}^H$ was only 1.44 ms at $\tau = 17.96$ μs (i.e., 2π rotation), about five times shorter than that using the LG spin lock scheme. This implies that the ^{1}H magnetization decays much faster along the magic angle under the FSLG sequence than during the simple LG sequence in spite of the fact that the former sequence suppresses the proton homonuclear dipolar interaction more efficiently than the latter one. When used in the spin exchange experiments, FSLG gives rise to considerably longer heteronuclear dipolar oscillation than the simple LG sequence (*24*). This can be explained by Eq. [2] that the damping of the heteronuclear dipolar oscillation is governed by $T_{1\rho}^H$ in the tilted rotating frame and the proton spin diffusion rate R. Therefore, although FSLG exhibits a short $T_{1\rho}^H$, it significantly decreases the proton spin diffusion by sufficiently suppressing the strong proton homonuclear dipolar interaction. When $\tau = 35.92$ μs (i.e., 4π rotation), $T_{1\rho}^H$ obtained was 2.53 ms, as shown in Fig. 2. Apparently, $T_{1\rho}^H$ under the FSLG sequence becomes longer with a slower flip-flop rate of the effective field. As discussed by Ramamoorthy *et al.* (*24, 25*), the phase transients during the flip-flop may result in a reduction of the spin locked signals. An additional π pulse has been introduced between the flip-flop to refocus the phase transient effect (*25*). Such phase transients have dramatic effects in multiple-pulse experiments such as CRAMPS (*26, 27*); thus it is essential to perform systematic tune-up procedures (*28–30*) to minimize the phase transient effects. In the FSLG sequence, the phase transients are only present in the beginning and the end of the pulse length of τ, especially for a relatively long pulse length, as in our experiments where τ was 17.96 and 35.92 μs, respectively. The phase transients deviate the effective field from the magic angle resulting in an imperfect spin lock field and eventually contribute to the loss of the spin locked magnetization. These phase transient effects in the PISEMA experiments may be minimized by a systematic tune-up procedure (*24*). However, in a separate experiment where the spectrometer was systematically tuned, a phenomenon similar to that in Fig. 2 was observed when using the phase ramp FSLG (unpublished results). Moreover, it was found that a shorter $T_{1\rho}^H$ was observed when the larger RF amplitude was used for FSLG (i.e., the shorter τ). Therefore, it is believed that, although the phase transients during the flip-flop of the effective field contribute to the loss of the spin lock signals, the significant reduction of the spin–lattice relaxation time $T_{1\rho}^H$ in the tilted rotating frame with the FSLG sequence actually results from the insufficient spin lock field. Figure 3 shows the ^{15}N spectra of the $^{15}N_{1,3,5,7}$-labeled gramicidin A in hydrated DMPC bilayers obtained from the pulse sequence of Fig. 1C with a fixed spin lock time of 862.08 μs. At $\tau = 17.96$ μs (i.e., 2π rotation with a total of 24 cycles), the ^{15}N signal intensity is considerably reduced compared to $\tau = 35.92$ μs (i.e., 4π rotation with a total of 12 cycles). The sign of the effective field changes twice in each cycle. Thus for a given spin lock time more cycles mean that the effective field alternates its direction more frequently. As a result, the magnetization decays faster. This was also observed in the simultaneous phase-inversion cross-polarization scheme (*31*). In fact, although the strong proton homonuclear dipolar interaction is sufficiently suppressed by the FSLG sequence, the net rotation of the RF field over each cycle is zero due to the 2π rotation of the opposite effective fields of the two LG units (*32, 33*). This implies that the average effective spin lock field over the FSLG cycles may become comparable with residual internal interactions in the system such as the field inhomogeneity and high-order homonuclear dipolar interactions, so that the spin lock becomes less efficient, thus leading to a short $T_{1\rho}^H$. It is anticipated that $T_{1\rho}^H$ in the tilted rotating frame of the FSLG

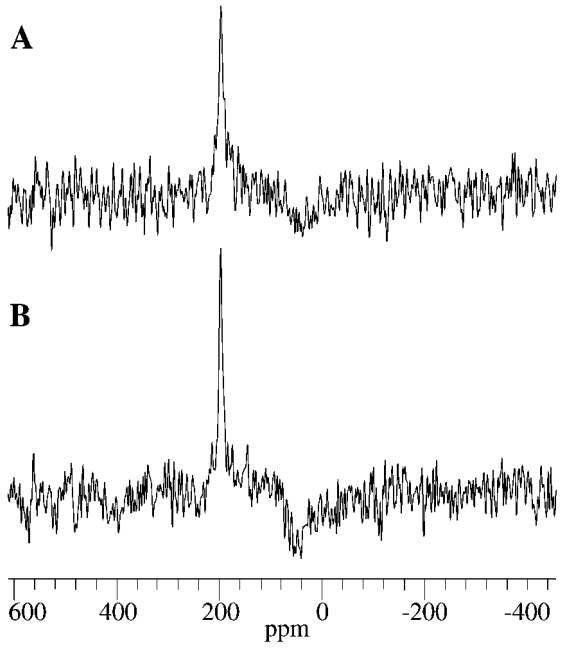

FIG. 3. ^{15}N spectra of the $^{15}N_{1,3,5,7}$-labeled gramicidin A obtained from the CMX 400 NMR spectrometer by using the pulse sequence shown in Fig. 1C with a constant spin lock time of 862.08 μs. The experimental parameters were the same as in Fig. 2 but using different effective field rotations for each LG unit: (A) $\tau = 17.96$ μs (i.e., 2π rotation) with a total of 24 cycles; (B) $\tau = 35.92$ μs (i.e., 4π rotation) with a total of 12 cycles.

may become even shorter with higher RF amplitude because a rapid phase alternation of the effective field may result in a better averaging of the RF spin lock field.

Figure 4A shows a standard pulse sequence for PISEMA experiments. Following a conventional cross polarization from protons to ^{15}N, the ^{1}H magnetization is spin locked by a FSLG sequence. At the same time, the phase of the spin lock field on the ^{15}N channel is alternated synchronously with the change of the effective field direction of the LG units in the FSLG sequence, enabling the coherent energy transfer between the protons and ^{15}N by cross polarization. The t_1 increment corresponds to an integral number of the FSLG cycles. In the end, the ^{15}N signals encoded with the ^{15}N–^{1}H heteronuclear dipolar interaction are detected under the high-power proton decoupling. In our experiments, the RF amplitude during t_1 (i.e., the FSLG period) was decreased in order to fulfill the cross-polarization matching condition without changing the ^{15}N RF amplitude because of ^{15}N amplifier limitations. Figure 4B shows the resulting PISEMA spectrum of the $^{15}N_{1,3,5,7}$-labeled gramicidin A in hydrated DMPC bilayers. The same ^{15}N–^{1}H dipolar interaction is expected for all these labeled sites, as indicated in the spectrum, because the ^{15}N labels with their attached ^{1}H have virtually the same orientation with respect to the magnetic field direction (*21, 22*). From a slice taken at 198 ppm along the dipolar dimension, as shown on the left, the dipolar linewidth of 980 Hz is obtained.

Figure 5A shows a modified pulse sequence for PISEMA experiments. Instead of using the LG_{+Y}-LG_{-Y} cycle of FSLG as in Fig. 4A, a supercycle of LG_{+Y}-LG_{-Y}-$LG_{-Y}LG_{+Y}$ is used in the FSLG sequence. Although it is not clear if such a supercycle performs better proton homonuclear dipolar decoupling, as is the case for the heteronuclear decoupling in solution NMR (*34*), it reduces the number of the phase alternations of the effective fields by half for a given spin lock time. In terms of the spin locking, the supercycle is essentially the same as using FSLG with 4π rotation. As discussed above, $T_{1\rho}^H$ in the tilted rotating frame under the FSLG sequence using 4π rotation was about twice as long as that using 2π rotation, as indicated in Fig. 2. And it is also applicable to the ^{15}N spin lock field. However, the effect of the ^{15}N spin lock on the quality of the PISEMA spectrum is less significant than that of the proton spin lock because the spin–lattice relaxation time $T_{1\rho}^N$ for ^{15}N in the tilted rotating frame is usually much longer than $T_{1\rho}^H$. Thus it is anticipated that a shorter $T_{1\rho}^H$ could result in a narrower linewidth in the dipolar dimension of the PISEMA spectra. Figure 5B shows the PISEMA spectrum of the $^{15}N_{1,3,5,7}$-labeled gramicidin A in hydrated DMPC bilayers using the pulse sequence in Fig. 5A. A

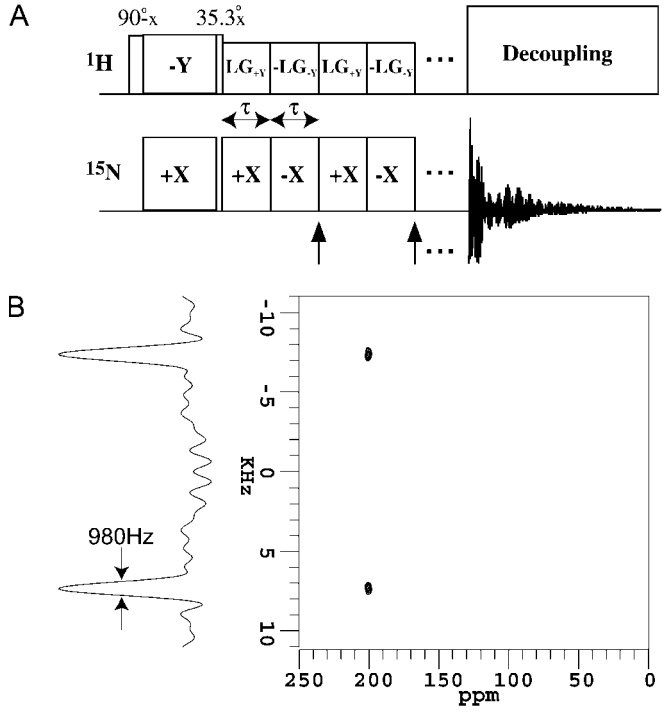

FIG. 4. (A) Two-dimensional (2D) PISEMA pulse sequence. The ↑ indicates the t_1 increment corresponding to an integral number of the FSLG cycle. (B) 2D PISEMA spectra of the $^{15}N_{1,3,5,7}$-labeled gramicidin A recorded on the CMX 400 at 310 K using the pulse sequence in (4A). On the left a slice taken at 198 ppm along the dipolar dimension is shown. The linewidth of 980 Hz at the half-height was measured and the dipolar splitting was scaled to 14.6 kHz. The ^{1}H RF amplitude used for cross polarization was 45.5 kHz and then decreased to 37.1 kHz in combination with a frequency jump of 26.3 kHz so as to fulfill the Hartmann–Hahn match during t_1 without changing the ^{15}N RF amplitude. For each LG unit $\tau = 22$ μs corresponding to a 360° rotation and resulting in a dwell time of 44 μs in the t_1 dimension. A total of 32 t_1 increments were recorded with a recycle delay of 7 s.

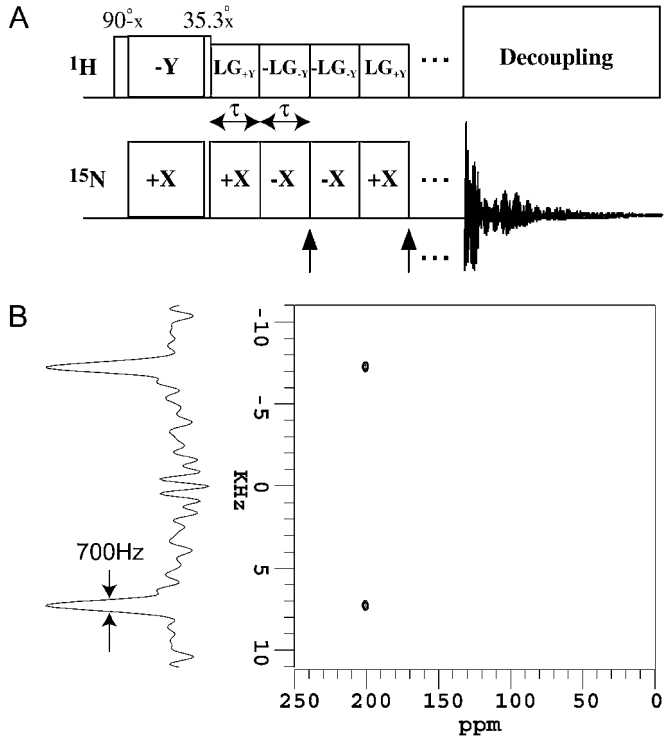

FIG. 5. (A) Modified 2D PISEMA pulse sequence. The ↑ indicates the t_1 increment corresponding to an integral number of the FSLG cycle. (B) 2D PISEMA spectra of the $^{15}N_{1,3,5,7}$-labeled gramicidin A recorded on the CMX 400 at 310 K using the pulse sequence in (5A). On the left a slice taken at 198 ppm along the dipolar dimension is shown. The linewidth of 700 Hz at the half-height was measured and the dipolar splitting was scaled to 14.6 kHz. The experimental parameters were the same as in Fig. 4B.

slice taken at 198 ppm along the dipolar dimension, as shown on the left, indicates a dipolar linewidth of 700 Hz, which is about a 30% improvement compared to the result from Fig. 4.

In conclusion, a rapid phase alternation of the effective field in the FSLG sequence results in averaging of the RF spin lock field so that the spin locking of the proton magnetization becomes less efficient and thus dramatically shortens the spin–lattice relaxation time $T_{1\rho}^H$ in the tilted rotating frame. Since the $T_{1\rho}^H$ in the tilted rotating frame may be directly associated with the dipolar linewidth in the PISEMA spectra, prolonging $T_{1\rho}^H$ could further improve resolution in the PISEMA spectra. It has been demonstrated that the dipolar linewidths in the PISEMA spectra can be reduced with the use of the simple supercycles in the PISEMA pulse sequence. Further pulse sequence development along this direction is currently under investigation.

ACKNOWLEDGMENTS

The authors are indebted to Dr. Z. Gan for helpful discussion. We also gratefully acknowledge helpful comments of a referee concerning the phase transient effects during the flip-flop of the FSLG spin lock field. This work was supported by the National Science Foundation MCB 9986036 and the work was largely performed at the National High Magnetic Field Laboratory supported by the National Science Foundation Cooperative Agreement DMR-0084173 and the state of Florida.

REFERENCES

1. M. Lee and W. Goldburg, Nuclear magnetic resonance line narrowing by a rotating RF field, *Phys. Rev.* **140,** 1261–1271 (1965).
2. A. Bielecki, A. C. Kolbert, H. J. M. de Groot, R. G. Griffin, and M. H. Levitt, Frequency-switched Lee–Goldburg sequences in solids, *Adv. Magn. Reson.* **14,** 111–150 (1990).
3. C. H. Wu, A. Ramamoorthy, and S. J. Opella, High-resolution heteronuclear dipolar solid-state NMR spectroscopy, *J. Magn. Reson. A* **109,** 270–272 (1994).
4. F. M. Marassi, A. Ramamoorthy, and S. J. Opella, Complete resolution of the solid-state NMR spectrum of a uniformly ^{15}N-labeled membrane protein in phospholipid bilayers, *Proc. Natl. Acad. Sci. USA* **94,** 8551–8556 (1997).
5. Y. Kim, K. Valentine, S. J. Opella, S. L. Schendel, and W. A. Cramer, Solid-state NMR studies of the membrane-bound closed state of the colicin E1 channel domain in lipid bilayers, *Protein Sci.* **7,** 342–348 (1998).
6. F. M. Marassi and S. J. Opella, NMR structural studies of membrane proteins, *Curr. Opin. Struct. Biol.* **8,** 640–648 (1998).
7. S. J. Opella, F. M. Marassi, J. J. Gesell, A. P. Valente, Y. Kim, M. Oblatt-Montal, and M. Montal, Structures of M2 channel-lining segments from nicotinic acetylcholine and NMDA receptors by NMR spectroscopy, *Nat. Struct. Biol.* **6,** 374–379 (1999).
8. Z. Song, F. Kovacs, J. Wang, J. Denny, S. C. Shekar, J. R. Quine, and T. A. Cross, Transmembrane domain of M2 protein from influenza A virus studied by solid-state ^{15}N polarization inversion spin exchange at magic angle NMR, *Biophys. J.* **79,** 767–775 (2000).
9. J. Wang, J. Denny, C. Tian, S. Kim, Y. Mo, F. Kovacs, Z. Song, K. Nishimura, Z. Gan, R. Fu, J. R. Quine, and T. A. Cross, Imaging membrane protein helical wheels, *J. Magn. Reson.* **144,** 162–167 (2000).
10. F. M. Marassi and S. J. Opella, A solid-state NMR index of helical membrane proteins structure and topology, *J. Magn. Reson.* **144,** 150–155 (2000).
11. A. Pines, M. G. Gibby, and J. S. Waugh, Proton-enhanced NMR of dilute spins in solids, *J. Chem. Phys.* **59,** 569–590 (1973).
12. S. R. Hartmann and E. L. Hahn, Nuclear double resonance in the rotating frame, *Phys. Rev.* **128,** 2042–2053 (1962).
13. L. Müller, A. Kumar, T. Baumann, and R. R. Ernst, Transient oscillations in NMR cross-polarization experiments in solids, *Phys. Rev. Lett.* **32,** 1402–1406 (1974).
14. R. Pratima and K. V. Ramanathan, The application to liquid crystals of transient oscillations in cross polarization experiments, *J. Magn. Reson. A* **118,** 7–10 (1996).
15. P. Palmas, P. Tekely, and D. Canet, Local-field measurements on powder samples from polarization inversion of the rare-spin magnetization, *J. Magn. Reson. A* **104,** 26–36 (1993).
16. F. Tian and T. A. Cross, Dipolar oscillations in cross-polarized peptide samples in oriented lipid bilayers, *J. Magn. Reson.* **125,** 220–223 (1997).
17. F. Tian, R. Fu, and T. A. Cross, ^{13}C selective polarization and spin diffusion in a lipid bilayer bound polypeptide by solid-state NMR, *J. Magn. Reson.* **139,** 377–381 (1999).
18. A. Bielecki, A. C. Bolbert, and M. H. Levitt, Frequency-switched pulse sequences: Homonuclear decoupling and dilute spin NMR in solids, *Chem. Phys. Lett.* **155,** 341–346 (1989).
19. Z. Gan, Spin dynamics of polarization inversion spin exchange at the magic angle in multiple spin systems, *J. Magn. Reson.* **143,** 136–143 (2000).
20. J. S. Waugh, Uncoupling of local field spectra in nuclear magnetic resonance: Determination of atomic positions in solids, *Proc. Natl. Acad. Sci. USA* **73,** 1394–1397 (1976).

21. R. Ketchem, W. Hu, and T. A. Cross, High-resolution conformation of gramicidin A in a lipid bilayer by solid state NMR, *Science* **261,** 1457–1460 (1993).

22. R. R. Ketchem, B. Roux, and T. A. Cross, High-resolution polypeptide structure in a lameller phase lipid environment from solid state NMR derived orientational constraints, *Structure* **5,** 1655–1669 (1997).

23. P. Tekely, P. Palmas, and D. Canet, Effect of proton spin exchange on the residual ^{13}C MAS NMR linewidth. Phase-modulated irradiation for efficient heteronuclear decoupling in rapidly rotating solids, *J. Magn. Reson. A* **107,** 129–133 (1994).

24. A. Ramamoorthy and S. J. Opella, Experimental aspects of multidimensional solid-state NMR correlation spectroscopy, *J. Magn. Reson.* **140,** 131–140 (1999).

25. A. Ramamoorthy and S. J. Opella, Two-dimensional chemical shift/heteronuclear dipolar coupling spectra obtained with polarization inversion spin exchange at the magic angle and magic-angle sample spinning (PISEMAMAS), *Solid State Nucl. Magn. Reson.* **4,** 387–392 (1995).

26. J. S. Waugh, L. M. Huber, and U. Haeberlen, Approach to high-resolution NMR in solids, *Phys. Rev. Lett.* **20,** 180 (1968).

27. W. K. Rhim, D. D. Elleman, and R. W. Vaughan, Enhanced resolution for solid state NMR, *J. Chem. Phys.* **58,** 1772 (1973).

28. D. P. Burum, M. Linder, and R. R. Ernst, A new "tune-up" NMR pulse cycle for minimizing and characterizing phase transients, *J. Magn. Reson.* **43,** 463–471 (1981).

29. B. C. Gerstein and C. R. Dybowski, "Transient Techniques in NMR of Solids: An Introduction to Theory and Practice," Academic Press, London (1985).

30. U. Haeberlen, "High Resolution NMR in Solids, Selective Averaging," Academic Press, New York (1976).

31. X. Wu and K. W. Zilm, Cross polarizaton with high-speed magic-angle spinning, *J. Magn. Reson. A* **104,** 154 (1993).

32. R. Fu, S. Caldarelli, V. Ermakov, and G. Bodenhausen, NMR of residual protons in partly deuterated anisotropic materials with phase-alternated decoupling of deuterium spins, *Solid State Nucl. Magn. Reson.* **5,** 273–291 (1996).

33. C. Counsell, M. H. Levitt, and R. R. Ernst, Analytical theory of composite pulses, *J. Magn. Reson.* **63,** 133–141 (1985).

34. M. H. Levitt, R. Freeman, and T. Frenkiel, Supercycles for broadband heteronuclear decoupling, *J. Magn. Reson.* **50,** 157–160 (1982).